HHS Public Access

Author manuscript

Cell. Author manuscript; available in PMC 2017 January 14.

Published in final edited form as:

Cell. 2016 January 14; 164(0): 246–257. doi:10.1016/j.cell.2015.11.051.

Extracellular vesicles from *Trypanosoma brucei* mediate virulence factor transfer and cause host anemia

Anthony J. Szempruch[1,7], **Steven E. Sykes**[1,7], **Rudo Kieft**[1], **Lauren Denison**[1], **Allison C. Becker**[1], **Anzio Gartrell**[1], **William J. Martin**[2], **Ernesto S. Nakayasu**[3], **Igor C. Almeida**[4], **Stephen L. Hajduk**[1,5,6], and **John M. Harrington**[1,5,6]

[1]Department of Biochemistry and Molecular Biology, University of Georgia, Athens, GA 30602

[2]Animal Health Research Center, University of Georgia, Athens, GA 30602

[3]Biological Sciences Division, Pacific Northwest National Laboratory, Richland, WA 99352

[4]Border Biomedical Research Center, Department of Biological Sciences, University of Texas, El Paso, TX 79968

Abstract

Intercellular communication between parasites and with host cells provides mechanisms for parasite development, immune evasion and disease pathology. Bloodstream African trypanosomes produce membranous nanotubes that originate from the flagellar membrane and disassociate into free extracellular vesicles (EVs). Trypanosome EVs contain several flagellar proteins that contribute to virulence and *Trypanosoma brucei rhodesiense* EVs contain the serum resistance-associated protein (SRA) necessary for human infectivity. *T. b. rhodesiense* EVs transfer SRA to non-human infectious trypanosomes allowing evasion of human innate immunity. Trypanosome EVs can also fuse with mammalian erythrocytes resulting in rapid erythrocyte clearance and anemia. These data indicate that trypanosome EVs are organelles mediating non-hereditary virulence factor transfer and causing host erythrocyte remodeling inducing anemia.

INTRODUCTION

Bacteria and eukaryotic cells use extracellular vesicles (EVs) as vehicles for delivery of modulatory proteins, lipids and nucleic acids to neighboring cells (Schorey et al., 2015;

[6]Co-corrisponding Authors: shajduk@bmb.uga.edu (SLH), johnmharrin@gmail.com (JMH).
[5]Co-senior Author
[7]Co-first Author

Author contributions

Conceptualization, A. J. S., S. E. S., S. L. H. and J. M. H.; Investigation, A. J. S., S. E. S., R. K., L. W. D., A. C. B., A. G., W. J. M., and J. M. H.; Resources, I. C. A.; Formal Analysis, E. S. N and I. C. A.; Writing – Original Draft, A. J. S., S. L. H. and J. M. H.; Writing – Review & Editing, All authors.

Raw LC-MS/MS runs and MaxQuant searching results were uploaded to PRIDE database (http://www.ebi.ac.uk/pride/) under accession number PXD002030.

Yanez-Mo et al., 2015). Extracellular vesicles generally fall into two classes: 1) exosomes produced in the exocytic pathways and generally associated with the formation of multivesicular bodies (MVBs) and 2) ectosomes formed by budding of the plasma membrane. Both carry effector proteins and nucleic acids (Schorey et al., 2015; Wood and Rosenbaum, 2015). Functions proposed for EVs include transfer of drug resistance, growth regulation, quorum sensing, immune regulation, developmental modulation and neurotransmission (Remis et al., 2014). In addition, several human diseases including cancer, atherosclerosis, neurodegeneration, as well as viral and parasite infections are affected by EV production. A clear and defining function of EVs is the delivery of modulatory molecules to other cells within and between species. The range of functions attributed to EVs is reflected in diverse mechanisms of EV biogenesis and composition (Schorey et al., 2015).

The kinetoplastidae is a diverse group of eukaryotic microbes responsible for several important human and animal diseases including African sleeping sickness (*Trypanosoma brucei rhodesiense* and *Trypanosoma brucei gambiense*), Chagas disease (*Trypanosoma cruzi*), Kala azar (*Leishmania donovani*) and Nagana in cattle (*Trypanosoma brucei brucei*). *T. cruzi* and *Leishmania* spp. have been shown to release EVs that interact with host cells and modulate immune responses (Marcilla et al., 2014). Other eukaryote pathogens also produce EVs. EVs derived from *Plasmodium falciparum*-infected erythrocytes promote parasite differentiation and regulate immune cells within the mammalian host (Mantel et al., 2013; Regev-Rudzki et al., 2013). The urogenital tract parasite *Trichomonas vaginalis* produces EVs that alter adherence to host cells and modulate the host immune response to infection (Twu et al., 2013).

Humans and other higher primates are innately immune to many African trypanosomes by virtue of circulating trypanosome lytic factors (TLF). Human pathogenic *T. b. rhodesiense* circumvents TLF activity through expression of a virulence factor, the serum-resistance associated protein (SRA) (De Greef and Hamers, 1994). The mechanism of SRA involves binding to apolipoprotein L-1 (ApoL-1), a pore forming toxin within TLF (Vanhamme et al., 2003). Binding, uptake and intracellular trafficking of TLF to early endosomes of *T. b. rhodesiense* leads to co-localization of SRA and TLF facilitating the neutralization of ApoL-1 activity(Stephens and Hajduk, 2011). Transfection of *T. b. brucei* with the gene encoding SRA or co-infection of tsetse flies with *T. b. rhodesiense* and *T. b. brucei* allows for transfer of the gene encoding *SRA* to *T. b. brucei* and confers resistance to TLF (Gibson et al., 2015; Xong et al., 1998). Direct transfer of this virulence protein between trypanosomes has not been reported.

Like many extracellular pathogens, African trypanosome infection initially elicits a type 1 immune response that includes expression of inflammatory cytokines and activation of myeloid cells. These host immune responses have been implicated in the pathology of trypanosomiasis-associated anemia (Stijlemans et al., 2015). Anemia is markedly severe during acute infection and is the major cause of cattle death due to Nagana (Naessens, 2006). Recently, erythrophagocytosis by activated liver and spleen myeloid cells has been identified as a major contributor to erythrocyte clearance. In addition, the lipid composition of erythrocytes is altered during trypanosome infection and these erythrocytes are

preferentially phagocytosed by the host's myeloid cells (Stijlemans et al., 2015). While host responses that contribute to anemia have been characterized, the parasite factors that elicit erythrocyte clearance are unknown.

Here we describe a dynamic class of membrane nanotubes that bud from the trypanosome flagellar membrane and vesicularize to form EVs. The proteome of these EVs is enriched for specific flagellar membrane proteins and contains a number of proteins implicated in virulence and persistence within the host. Functionally we show that *T. brucei* EVs fuse with target lipid bilayers, including the flagellar pocket of neighboring trypanosomes, resulting in transfer and internalization of lipids and proteins. Transferred proteins retain activity since *T. b. rhodesiense* EVs transfer SRA to *T. b. brucei* resulting in resistance to TLF. *T. brucei* EVs are also highly fusogenic with host erythrocyte membranes, altering the physical properties of the membrane and causing erythrocyte clearance from circulation. We postulate that this causes anemia during animal and human infection by African trypanosomes. Our findings show that EVs contribute to the complexity of African trypanosomiasis through the transfer of virulence factors between parasites and inadvertent interaction with host cells, which has a profound effect on disease.

RESULTS AND DISCUSSION

Flagellar membrane budding gives rise to nanotubes and EVs in *T. brucei*

Exchange of metabolites, nucleic acids and proteins in bacteria can take place over short and long distances via the formation of membrane nanotubes between individual bacterium and production and delivery of EVs (Dubey and Ben-Yehuda, 2011). Cell-cell communication occurs in the eukaryotic pathogen *T. b. brucei* as demonstrated by quorum sensing-mediated differentiation into the tsetse fly transmissible short-stumpy developmental form in the mammalian bloodstream (Mony et al., 2014) and social motility exhibited by procyclic forms in the insect vector midgut (Oberholzer et al., 2010). The molecular mechanisms underlying these communication processes in African trypanosomes have not yet been identified.

Visualization of bloodstream form (BF) *T. b. brucei* by differential interference contrast (DIC) video microscopy revealed the presence of highly dynamic filamentous structures (2–20 μm) extending from the posterior end of some cells (Figure 1A). These structures resembled previously described thread-like appendages, later called plasmanemes, associated with BF African trypanosomes (Babudieri and Tomasini, 1962; Schepilewsky, 1912; Vickerman and Luckins, 1969). Occasionally filaments appeared to make connections with the posterior ends of other trypanosomes and if unattached become highly branched (Figure 1A). These structures were largely disregarded due to lack of detection from blood of infected mice (Ellis et al., 1976; Wright et al., 1970). To determine if these structures were physiologically relevant we performed DIC video microscopy of infected mouse blood. Similar filamentous structures were also visible on *T. brucei* in the blood of infected mice (Figures 1B and S1A). The formation of the filaments *in vitro* was stimulated by stress from RNAi against an essential BF protein or by addition of complement active serum to growth medium (Figure S1B) (Sykes et al., 2015). These induction mechanisms allowed us to investigate filament biogenesis.

Live imaging of BF *T. brucei* labeled with the membrane binding dye octadecyl rhodamine B (R18) suggested that filaments were bounded by a lipid membrane and led us to rename the plasmanemes “membrane nanotubes” to better reflect their structure and composition (Figure 1C, Movie S1 and S2). Observations of nanotubes connecting cells showed these interactions were stable over long distances (>20 μm) and highly dynamic, releasing and forming new connections with several cells over time (Figure 1D and Movie S3). When visualized by negative stain transmission electron microscopy (TEM), nascent nanotubes showed a continuous membrane (Figure 1E and Figure S1C), consistent with previous observations using negative stain and thin section TEM (Frevert and Reinwald, 1988; Vickerman and Luckins, 1969). Though it has been shown previously that short stumpy *T. brucei* produce “secretory-filaments” we restricted our studies to exponentially growing long slender BF *T. brucei* (Ellis et al., 1976). Nanotubes were restricted to the cell posterior, suggesting a polarized point of origin. TEM of thin sections revealed membrane budding from the flagellum, with similar characteristics to the adjacent flagellar membrane (Figure 1F and Figure S1D) and three-dimensional reconstruction of serial sections showed that protrusion of the flagellar membrane gave rise to a tubular structure lacking the axoneme and paraflagellar rod (Figure 1G and Movie S4). These observations suggested that *T. brucei* nanotubes developed from budding of the flagellar membrane and extended for at least a short distance parallel to the flagellum. Longitudinal sections through nanotubes revealed repeating spherical units resembling “beads on a string” outside the flagellar pocket at the cell surface (Figure 2A). The average diameter of a “bead” was approximately 100 nm (Figure 2B). The vesicular appearance of trypanosome nanotubes resembles the vesicle chains that dissociate to produce free EVs in the bacterium *Myxococcus xanthus* (Dubey and Ben-Yehuda, 2011). These observations are similar to previous reports from trypanosomes (Babudieri and Tomasini, 1962; Ellis et al., 1976; Frevert and Reinwald, 1988; Schepilewsky, 1912). Indeed, scanning electron microscopy revealed trypanosome-associated vesicles consistent in size with nanotube beads (Figure 2C). Using DIC video microscopy, we observed the dynamics of formation, release and disassociation of a nanotube into diffusible EVs (Figure 2D and Movie S5). Release from nanotubes allowed us to purify, characterize and investigate the cellular interactions of trypanosome EVs derived from exponentially growing cells, that have not been stimulated for nanotube formation.

The EV proteome is enriched in flagellar membrane proteins and parasite virulence factors

When viewed by negative stain TEM purified EVs appear as unilamellar vesicles approximately 70–80 nm in diameter, consistent with the size of nanotube associated beads (Figure 2E upper panel). TEM thin section analysis of purified EVs revealed membrane-bound vesicles of ~80 nm in size with a 10 nm thick membrane (Figure 2E lower panel and Figure S1E) with similar characteristics to cell plasma membrane (Figure S1F). Nanoparticle tracking analysis revealed a major population of vesicles with a mean diameter of 81 nm and a minor population 165 nm in diameter (Figure 2F). Purified EVs showed a different SDS-PAGE protein profile than total cell (Figure. 2G). Proteomic analysis of EVs revealed 156 proteins from diverse functional classes (Table S1) and several were confirmed by western blotting, including the expressed variant surface glycoprotein (VSG 221), Hsp-70, glycerol kinase and aldolase (Figure 2H). Similar to observations from *Leishmania* spp. we detected ribosomal proteins in the *T. brucei* EV proteome (Silverman et al., 2010).

Although it is not uncommon to screen out proteins based on high isoelectric point, removing many ribosomal proteins, we performed an analysis on the complete/unfiltered 156 proteins (Figure 2I, Table S1 and Table S2) (Broadhead et al., 2006). Comparison of the EV proteome with that of the flagellar surface and flagellar matrix showed significant overlap (Figure 2I) (Oberholzer et al., 2011). Our analysis showed that 50 of 156 EV proteins were either flagellar matrix or membrane proteins representing 32% of the EV proteome. In addition, we found only minor similarity with the glycosome (2%) and mitochondrial (2%) proteomes (Guther et al., 2014; Panigrahi et al., 2009) (Figure 2I and Table S2), which is proportionally similar when compared to the total proteome; therefore, EVs from *T. b. brucei* BFs are not enriched with proteins from these two organelles. Ten of these proteins have previously been co-localized by fluorescence microcopy and were shown to be flagellar/flagellar-associated (Table S2). While the EVs appear homogeneous in size and morphology they may be derived from multiple mechanisms of origin. Enrichment of EVs with flagellar proteins is consistent with a population of EVs being derived from nanotubes that form by budding of the flagellar membrane. We observed that in addition to abundant proteins such as VSG more than 20% of the EVs composition was from low abundance proteins (Table S2) (Jensen et al., 2014). Among these minor proteins were several flagellar proteins, including calflagin (CF), adenylate cyclase (GRESAG4), glycosylphosphatidylinositol phospholipase C (GPI-PLC) and metacaspase 4 (MCA4), that contribute to the virulence of *T. brucei* in the mammalian host (Table S2) (Emmer et al., 2010; Proto et al., 2011; Salmon et al., 2012; Webb et al., 1997). We next determined whether African trypanosomes expressing SRA, a well-characterized virulence factor, release EVs containing this protein. Extracellular vesicles were purified from a *T. b. brucei* line expressing a Ty-epitope tagged SRA (*T. b. brucei*$^{SRA\text{-}Ty}$) (Oli et al., 2006) and western blots demonstrated the presence of SRA in these preparations (Figure 2J). The diversity of virulence factors detected in the EV proteome suggests that the flagellum may serve as part of a sorting pathway for delivery of biologically active molecules to neighboring cells.

T. b. rhodesiense EVs transfer SRA to *T. b. brucei* and confers resistance to TLF

The observation that SRA was present in EVs led us to investigate whether SRA could be transferred to TLF susceptible *T. b. brucei*. We used flow cytometry to determine whether EVs from *T. b. brucei*$^{SRA\text{-}Ty}$ bound and were taken-up by wild type *T. b. brucei* (Figures 3A and 3B). *T. b. brucei* were incubated with SRA-Ty containing EVs at 37°C, washed to remove unbound EVs and fixed with paraformaldehyde. Fixed cells were either treated directly with anti-Ty antibody and a fluorescent secondary antibody (Figure 3A) or first treated with low concentrations of detergent (0.1% Triton X-100) to permeabilize the cells prior to addition of antibodies (Figure 3B). EV treated wild type *T. b. brucei* became SRA-Ty positive after detergent treatment. Suggesting that EVs delivered SRA-Ty which accumulated in an intracellular location that was accessible to antibodies only following detergent permeabilization. Immunofluorescence microscopy indicated that SRA-Ty delivered by EVs was internalized by wild type *T. b. brucei* and co-localized with concanavalin A (ConA) a marker for the trypanosome endocytic pathway (Figure 3C and S2A–C). Together these data indicated that SRA from EVs was deposited in the endolysosomal system of recipient trypanosomes. Since SRA localizes to endosomes in *T. b.*

rhodesiense and *T. b. brucei*$^{SRA\text{-}Ty}$ these observations suggested EV transfer of SRA may protect recipient *T. b. brucei* from TLF killing (Stephens and Hajduk, 2011).

There have been a number of reported human infections by non-human infectious species of trypanosomes (Truc et al., 2013). While these may represent either misidentification of the parasite or genetic acquisition of TLF resistance, an alternative possibility is transfer of SRA to TLF susceptible trypanosomes during a dual infection with *T. b. rhodesiense*. Our discovery that SRA was transferred by EVs to *T. b. brucei* and localized to an endolysosomal compartment led us to ask whether co-cultivation of *T. b. brucei* $^{SRA\text{-}Ty}$ or *T. b. rhodesiense* with wild type *T. b. brucei* conferred TLF resistance (Figures 3D–F and S2D). Co-cultivation of *T. b. brucei* $^{SRA\text{-}Ty}$ and *T. b. brucei*^{Hyg} allowed selection of a small (20%) but reproducible fraction of cells showing dual resistance to TLF and hygromycin (Figure S2D). In order to avoid the long selection time needed for the outgrowth of hygromycin resistant cells, recipient *T. b. brucei* were cultured in a transwell system separated by a 0.2 μm filter from either *T. b. brucei* $^{SRA\text{-}Ty}$ or *T. b. rhodesiense*. The transwell membrane prevented direct contact between the donor and recipient cells but allowed diffusion of EVs into the compartment containing the recipient *T. b. brucei* (Figure 3D). Co-cultivation of *T. b. brucei* opposite *T. b. brucei* $^{SRA\text{-}Ty}$ or *T. b. rhodesiense* in transwells led to an increase in TLF resistant *T. b. brucei* with the percentage of cells surviving overnight incubation with TLF approaching levels observed for untreated cells (Figures 3E and 3F).

While these co-cultivation studies were consistent with EV transfer of SRA to recipient cells they did not exclude the possibility that diffusible, non-EV-associated SRA could cross the transwell membrane conferring TLF resistance to the recipient cells. To exclude this possibility purified EVs were added directly to wild type *T. b. brucei* (Figure 3G). Addition of EVs from *T. b. brucei*$^{SRA\text{-}Ty}$ or *T. b. rhodesiense* but not EVs from wild type *T. b. brucei* increased TLF resistance of recipient *T. b. brucei* in a dose-dependent manner (Figures 3H, 3I and S2E). These data indicated that functional SRA was transferred by EVs to co-cultured trypanosomes leading to resistance to TLF.

Trypanosome EVs are highly fusogenic and rapidly transfer proteins and lipids to recipient trypanosomes

Internalization of EV-associated SRA by recipient *T. b. brucei* could be by receptor-mediated or fluid-phase endocytosis of EVs or may reflect direct fusion of EVs with the trypanosome plasma membrane. To determine the site of interaction and subsequent fate of EV proteins we labeled purified trypanosome EVs with Alexa-Fluor594 and followed the binding and localization of these proteins in *T. brucei*. When endocytosis was blocked, by maintaining cells at 3°C, EV proteins accumulated in the flagellar pocket as indicated by co-localization with ConA (Figure 4A). Binding of EVs to the trypanosome flagellar pocket was nonsaturable, suggesting a receptor-independent process (Figure S3A). This *T. brucei* EV binding could not be competed away with unlabeled BF *T. brucei* EVs (Figure S3B–C) or with EVs from a different life cycle stage (Figure S3D–E), related kinetoplastid *Leishmania tarentolae* (Figure S3F–G) or with human erythrocyte microvesicles (Figure S3H–K). After warming to 37°C, to allow endocytosis, both ConA and labeled EV proteins

localized within endolysosomal vesicles (Figure 4B). *T. b. brucei* EVs bound and were taken up independent of the expressed VSG (Figure S4A) and subspecies of *T. brucei* (Figure S4B).

Since EV binding and uptake by *T. b. brucei* was receptor-independent and because EVs from other cell types have been shown to fuse with target cell membranes (Evans et al., 2012; Vidal and Hoekstra, 1995), we asked whether *T. brucei* EVs were fusogenic. Trypanosome EVs were purified and labeled with a self-quenching concentration of the lipophilic fluorophore octadecyl rhodamine B (R18). When R18-labeled EVs were incubated with *T. brucei*, a time-dependent increase in fluorescence was observed, indicating dilution of the fluorophore and suggesting fusion of the EVs with *T. brucei* membranes (Figure 4C). When visualized by ImageStream flow-cytometry, the R18 signal appeared initially localized to the posterior ends of cells and subsequently spread over the entire surface of the cell (Figures. 4D, 4E and S4C). These data are consistent with EVs fusing to the flagellar pocket membrane and rapid equilibration of EV lipids throughout the trypanosome membranes.

Trypanosome EVs are fusogenic with artificial liposomes and mammalian erythrocytes

To determine whether EV fusion was due to unique features of the flagellar pocket membrane of trypanosomes, purified R18-labeled *T. b. brucei* EVs were incubated with unlabeled 1-palmitoyl-2-oleoyl-sn-glycero-3-phosphocholine (POPC) large unilamellar liposomes (LUV). A time-dependent increase in fluorescence was observed as R18 was diluted into the unlabeled LUV membranes due to fusion (Figure 5A). Trypsinization of EVs ablated fusion, but EVs retained R18 loading requiring detergent treatment for R18 release, indicating that a(n) exposed EV protein(s) was necessary for membrane fusion (Figure 5A).

Since *T. b. brucei* is an extracellular parasite within the circulatory system, host erythrocytes would present abundant target membranes for EV fusion. Therefore we investigated whether *T. b. brucei* EVs fuse with mammalian erythrocytes. Purified EVs, but not POPC LUV, fused with human erythrocyte ghosts and fusion was ablated by trypsinization of the EV (Figure 5B). Flow cytometry indicates that EVs fuse with intact erythrocytes and transfer R18 from EVs to erythrocytes (Figure 5C). Fluorescence microscopy of R18-EV treated erythrocytes revealed a diffuse R18 signal spread over the surface of the cell (Figure 5D). Fusion also resulted in transfer of Alexa-Fluor labeled EV proteins to erythrocytes (Figure 5E). Therefore, EVs facilitate transfer of trypanosome lipid and protein to host erythrocytes. To further address this possibility, BF *T. b. brucei* were labeled with R18, incubated with erythrocytes separated in 0.2 μm transwells and erythrocytes analyzed by flow cytometry (Figure 5F). Consistent with *T. b. brucei* EVs transfer, we found that erythrocytes became labeled with R18 under these conditions.

T. b. brucei EV fusion modifies erythrocytes and causes anemia

Rifkin demonstrated that membrane-form VSG was transferred to erythrocytes co-cultured with *T. b. brucei* (Rifkin and Landsberger, 1990). Based on the presence of VSG in EVs and transfer of EV proteins to erythrocytes, we asked whether VSG is present on EV treated

erythrocytes. Immunofluorescence microscopy showed VSG on the surface of erythrocytes treated with *T. b. brucei* EVs (Figure 6A). This result was recapitulated when erythrocytes were co-incubated with *T. b. brucei* separated in transwells, again consistent with the biogenesis and fusion of EVs (Figure 6B). Based on these results we postulate that fusogenic trypanosome EVs may serve as vehicles for pathogen-to-host cell transfer of membrane proteins.

Because EV fusion incorporates exogenous proteins and lipids into erythrocytes, we investigated whether the physical properties of the plasma membrane were altered. Human erythrocytes treated with EVs were less sensitive to osmotic lysis (Figure 6C). To more specifically define the EV-mediated changes to erythrocyte membranes, we probed plasma membrane lipid packing. Human erythrocytes incubated with EVs showed an increase in membrane rigidity as indicated by a narrowing and shift of the emission spectra of Laurdan towards shorter wavelengths (Figure 6D). Recently it has been shown that erythrocyte lipid composition was altered during trypanosomiasis, and these cells were preferentially phagocytosed by myeloid cells (Stijlemans et al., 2015). Incorporating parasite lipid via EV fusion may explain altered erythrocyte lipid composition.

Trypanosome infection elicits a severe loss of erythrocytes during acute phase infection that is independent of B-cell response or IgM (Magez et al., 2008). We found that during acute infection mice exhibited a level of anemia that correlates to parasitemia (Figures 6E and 6F). These data suggested that anemia during the acute phase was a response to a density dependent trypanosome factor. We reasoned that EVs would be present at concentrations dependent on parasite density and that EV altered erythrocytes would be cleared from circulation. To test whether EV fusion causes clearance we incubated GFP-expressing mouse erythrocytes with *T. brucei* EVs and intravenously injected these cells into naive mice. Similar to human erythrocytes, EVs fuse with mouse erythrocytes and acquire VSG, lipid and increased rigidity (Figure S5A–D). Clearance occurred rapidly, within 1 hour, and the remaining EV treated erythrocytes became stable in circulation after 24 hr (Figure 6G). Finally, we tested whether circulating EVs stimulated a loss of erythrocytes. Injection of EVs into the tail vein of BALB/c or C57BL/6 mice resulted in increased erythrocyte volume (Figure S5E), which may be a consequence of lipid incorporation into the plasma membrane via EV-fusion, and a mean 5.3 % and 10.6 % decrease of erythrocytes (normalized to control injections) 1 hr post-injection (Figure 6H). These decreases correspond to a loss of 3.0×10^8 and 7.1×10^8 erythrocytes in BALB/C and C57BL/6 mice, respectively. Greater loss of erythrocytes in C57BL/6 is consistent with more severe anemia in trypanosome infected C57BL/6 than BALB/c mice (Magez et al., 2008). These data combined suggest that the fusogenic properties of trypanosome EVs directly alter the physical properties of erythrocytes and likely contribute to anemia associated with both cattle and human trypanosomiasis.

Concluding Remarks

It has become increasingly clear that most cells communicate within their immediate environment by the formation of membrane nanotube-like extensions and by the release of EVs (Remis et al., 2014; Schorey et al., 2015). Extracellular vesicles derived from “donor

cells" can have profound effects on "recipient cells" by altering gene expression and modulating signaling pathways resulting in developmental changes and modulation of immune response. EVs have also been shown to transfer virulence factors from infectious microbes to host cells, transmit infectious prion proteins and HIV and contribute to cancer and cardiovascular disease progression (Fevrier et al., 2004; Zomer et al., 2015). Here we report the discovery of EVs formed by the budding and subsequent vesicularization of long membrane nanotubes from the flagellum of African trypanosomes. In these studies we observed that *T. b. brucei* EVs contained several proposed trypanosome virulence factors. Furthermore, we showed that during co-cultivation EVs from *T. b. rhodesiense* facilitated the transfer of the virulence factor SRA to *T. b. brucei* where it localized within an endolysosomal compartment and conferred resistance to TLF. The formation of EVs was enhanced under stress conditions or with the addition of complement active serum and we postulate that EV delivery of virulence factors, including but not limited to SRA, might be advantageous to the parasite in immune competent hosts. We also found that trypanosome derived EVs are highly fusogenic with mammalian erythrocytes, resulting in physical changes to the erythrocyte membrane and rapid clearance in a mouse model. Anemia is associated with both human and cattle trypanosomiasis contributing to pathology and death.

Several proposed *T. b. brucei* virulence factors were found in the EV proteome, including the flagellar proteins GPI-PLC, calflagins, and metacaspase 4. While these proteins contribute to parasite virulence their mechanisms are unknown (Emmer et al., 2010; Proto et al., 2011; Webb et al., 1997). We found that nanotubes and EVs associated with trypanosomes have a thick VSG coat consistent with budding from the flagellar membrane; however purified EVs have a sparse coat suggesting activation of the EV associated GPI-PLC (Figures 2E and S1D, E). This may have implications in fusion of EVs with target membranes. *T. b. brucei* EVs also contained a flagellar adenylate cyclase (GRESAG4) previously proposed to increase the levels of cAMP in host immune cells, which in turn activates the host cell protein kinase A (PKA) (Salmon et al., 2012). The activation of host cell PKA reduced production of TNF-alpha sparing trypanosomes from host innate immunity (Salmon et al., 2012). While an appealing model, it was unclear how trypanosome adenylate cyclase could be transferred to host cells in an active state. Our discovery that highly fusogenic *T. b. brucei* EVs contain this enzyme raises the possibility that transfer of active GRESAG4 via EVs increased the levels of cAMP in recipient host cells.

The expression of SRA is necessary for human infectivity by *T. b. rhodesiense* and can be transferred to *T. b. brucei* during sexual crosses of the two subspecies in the tsetse fly vector (Gibson et al., 2015). This has important implications in the generation of new genetic variants of human infective trypanosomes. Parasite co-infection in tsetse flies is dependent on dual infection of the blood meal from the mammalian host with the two subspecies. While both *T. b. rhodesiense* and *T. b. brucei* can infect cattle and wild game it has been largely held that *T. b. brucei* cannot infect primates. We have shown that co-culturing the two subspecies resulted in transfer of SRA to *T. b. brucei* and the transmission of nonhereditary resistance to human TLF. This may have important implications in establishing dual infections in the tsetse fly and the generation of genetic diversity during

epidemics of sleeping sickness when humans would represent a significant reservoir of the parasites.

Anemia is a consistent symptom of human and veterinary trypanosomiasis and a major cause of morbidity (Naessens, 2006). The role of anemia in the pathology of trypanosomiasis cannot be overstated and it has been argued that the ability to resist anemia is more important for survival and reproduction than the ability to control parasitemia (Naessens, 2006). A pronounced anemia that is associated with a type 1 inflammatory response and erythrophagocytosis occurs during the acute phase of infection, whereas the significant, yet less severe anemia during the chronic phase coincides with a type 2 macrophage status and presence of the anti-inflammatory cytokine IL-10. The host responses that result in anemia are well characterized (Stijlemans et al., 2015). Our studies show that trypanosome EVs fuse with mammalian erythrocytes and cause changes to the physical properties of the membrane. We propose that our animal studies show that these changes lead to erythrophagocytosis and is the cause of anemia during acute trypanosomiasis. This discovery opens the possibility of identifying inhibitors of EV fusion with host cells and may lead to development of drugs that will spare the host from disease induced anemia.

FOR DETAILED PROCEDURES SEE SUPPLEMENTAL EXPERIMENTAL PROCEDURES

Trypanosome cell culture

Bloodstream form *T. b. brucei* Lister 427 (MiTat1.2) and *T. b. rhodesiense* KETRI2482 were grown in HMI-9 medium containing 10% fetal bovine serum (FBS) (Sigma) and Serum Plus supplement (SAFC Biosciences) in 5 % CO_2 at 37°C.

Nanotube and extracellular vesicle induction

Production of nanotubes and EVs was stimulated by stressing BF *T. brucei* with RNAi against the essential BF protein α-KDE1 or by the addition of complement active FBS (Sykes et al., 2015). In all other experiments, EVs were acquired from trypanosomes grown in heat inactivated serum or serum free conditions (for mass spectrometry).

Extracellular vesicle purification

T. brucei was grown in HMI-9 to a density of 1×10^6 cells/ml and EVs were purified as previously described with slight modification to the protocol (Bayer-Santos et al., 2013).

Human erythrocytes

Erythrocytes were removed by centrifugation, washed and stored in sterile PBS with 5 % dextrose, 0.5 mM EDTA.

Microscopy

All DIC and immunofluorescence images were acquired with a Zeiss Axio Observer Z1 as previously described Sykes et al., 2015.

Scanning and transmission electron microscopy

BF *T. brucei* stimulated for the formation of membrane nanotubes were fixed and images were acquired with a JEOL-JEM 1210 transmission electron microscope as previously described (Sykes et al., 2015). For SEM, 2.5% glutaraldehyde-fixed cells were dehydrated on a 0.22 mm membrane, critical point dried, sputter coated with gold and visualized with a Zeiss 1450EP scanning electron microscope. Three-dimensional reconstruction of serial TEM sections was carried out using tools available in the IMOD 4.7 software package (Kremer et al., 1996).

Nanoparticle tracking analysis

The concentration and diameter of freshly prepared EVs from 2×10^8 trypanosomes was determined by analysis with a NanoSight NS300 (Malvern). Fifteen hundred frames were acquired at 25 frames per second at 25°C.

SDS-PAGE and Western blotting

Total cell and purified EV proteins were fractionated by reducing SDS-PAGE and western blotted as previously described using 5×10^5 BF trypanosomes or EVs purified from 2×10^6 cells (Sykes et al., 2015).

SRA transfer assay

For flow cytometry, *T. brucei* was incubated with EVs for 1 hr at 37°C. *T. brucei*, *T. brucei*$^{SRA\text{-}Ty}$ and EV treated *T. brucei* cells were chilled washed with 1 x PBS, fixed with 0.05% paraformaldehyde and an aliquot was permeabilized with ice cold 0.1% Triton X-100. For microscopy *T. brucei* was incubated with EVs for 1 hr at 3°C or 30 min at 37°C. ConA was added and cells were prepared for fluorescence microscopy.

Overnight survival assay

Co-cultured or transwell co-cultured trypanosomes were treated with TLF for 24 hours at 37°C. Trypanosomes were incubated with purified EVs for 1 hr and then treated with TLF for 24 hr at 37°C. After treatment surviving cells were counted by phase-contrast microscopy and compared against non-TLF treated cultures.

EV protein transfer

Purified EVs were labeled with an Alexa-594 labeling kit (Life Technologies) and 1×10^7 cell equivalents were added to 1×10^8 *T. brucei* at 3°C. After washing cells were warmed to 37°C and prepared for microscopy (Sykes et al., 2015).

Membrane fusion assay

Vesicle fusion was measured essentially as described by Vidal and Hoekstra (1995).

Transwell co-culture

T. brucei was co-cultured with *T. brucei* $^{SRA\text{-}Ty}$ or *T. b. rhodesiense* in 0.2 μm transwell culture plates. Cells were co-cultured for 24 hours then split 1/10 and treated with TLF for

an overnight survival assay. For erythrocyte co-culture, *T. brucei* was inoculated with mouse or human erythrocytes in transwell plates.

Flow cytometry analysis of lipid and VSG transfer

After co-culture with trypanosomes, erythrocytes were washed prior to analysis. Samples analyzed for lipid transfer by R18 staining were directly analyzed while erythrocytes analyzed for VSG transfer were first treated using the protocol for fluorescence microscopy staining. All samples were then analyzed using a CyAn ADP Analyzer.

Osmotic lysis assay

Freshly collected human erythrocytes were resuspended in PBS and incubated with EVs. Erythrocytes were incubated in NaCl solutions, pelleted and the absorbance of the supernatant was read. Complete lysis was achieved by incubation in deionized H_2O.

Laurdan spectral analysis

Freshly collected human or mouse erythrocytes were resuspended in and incubated with EVs for 30 min. Erythrocytes were washed, labeled with Laurdan for 30 min, washed three times with PBS and spectra recorded with the Perkin Elmer Life Sciences LS-55 luminescent spectrofluorometer.

Trypanosome infections and EV treatments

Trypanosome infections were initiated by intraperitoneal injection of *T. b. brucei* Lister 427–221 parasites in retired breeder female BALB/c mice (Jackson Laboratory). Parasitemias were determined by the matching method (Herbert and Lumsden, 1976).

For *ex vivo* EV-treatment, erythrocytes from 10 week old mice expressing GFP from a ubiquitin promoter (C57BL/6-Tg(UBC-GFP)30Scha/J) (Jackson Laboratory) were collected and incubated with or without EVs. Erythrocytes were injected into the tail vein of naive C57BL/6J mice. Whole blood collected from the tail vein was analyzed by flow cytometry and GFP-positive erythrocytes were quantified from the ratio of labeled to unlabeled erythrocytes.

For direct EV injections, wild-type BALB/c and C57BL/6J mice were injected intravenously (tail vein) with EVs freshly prepared in PBS. Control mice were injected with an equal volume of PBS. Erythrocyte counts were determined via Coulter counting.

Supplementary Material

Refer to Web version on PubMed Central for supplementary material.

Acknowledgments

This work was supported by NIH grant AI039033 (S. L. H.) and 2G12MD007592 (BBRC/UTEP, I. C. A.). A.J.S. is supported in part by NIH training grant AI060546. We thank Amy Styer for reagents, Julie Nelson (University of Georgia) and Aaron Rae (Emory University) for assistance with flow cytometry, John Shields and Mary Ard (University of Georgia) for assistance with electron microscopy, the Biomolecule Analysis Core Facility at BBRC/UTEP (2G12MD007592) for the proteomic analysis and Ragy Ragheb for use and assistance with the NanoSight NS300.

References

Babudieri B, Tomasini N. Fine struttura dei trypanosomi. Parassitologia. 1962; 4:89–95.

Bayer-Santos E, Aguilar-Bonavides C, Rodrigues SP, Cordero EM, Marques AF, Varela-Ramirez A, Choi H, Yoshida N, da Silveira JF, Almeida IC. Proteomic analysis of Trypanosoma cruzi secretome: characterization of two populations of extracellular vesicles and soluble proteins. J Proteome Res. 2013; 12:883–897. [PubMed: 23214914]

Broadhead R, Dawe HR, Farr H, Griffiths S, Hart SR, Portman N, Shaw MK, Ginger ML, Gaskell SJ, McKean PG, et al. Flagellar motility is required for the viability of the bloodstream trypanosome. Nature. 2006; 440:224–227. [PubMed: 16525475]

De Greef C, Hamers R. The serum resistance-associated (SRA) gene of Trypanosoma brucei rhodesiense encodes a variant surface glycoprotein-like protein. Mol Biochem Parasitol. 1994; 68:277–284. [PubMed: 7739673]

Dubey GP, Ben-Yehuda S. Intercellular nanotubes mediate bacterial communication. Cell. 2011; 144:590–600. [PubMed: 21335240]

Ellis DS, Ormerod WE, Lumsden WH. Filaments of Trypanosoma brucei: some notes on differences in origin and structure in two strains of Trypanosoma (Trypanozoon) brucei rhodesiense. Acta Trop. 1976; 33:151–168. [PubMed: 8975]

Emmer BT, Daniels MD, Taylor JM, Epting CL, Engman DM. Calflagin inhibition prolongs host survival and suppresses parasitemia in Trypanosoma brucei infection. Eukaryot Cell. 2010; 9:934–942. [PubMed: 20418379]

Evans AG, Davey HM, Cookson A, Currinn H, Cooke-Fox G, Stanczyk PJ, Whitworth DE. Predatory activity of Myxococcus xanthus outer-membrane vesicles and properties of their hydrolase cargo. Microbiology. 2012; 158:2742–2752. [PubMed: 22977088]

Fevrier B, Vilette D, Archer F, Loew D, Faigle W, Vidal M, Laude H, Raposo G. Cells release prions in association with exosomes. Proc Natl Acad Sci U S A. 2004; 101:9683–9688. [PubMed: 15210972]

Frevert U, Reinwald E. Formation of filopodia in Trypanosoma congolense by crosslinking the variant surface antigen. J Ultrastruct Mol Struct Res. 1988; 99:124–136. [PubMed: 3171247]

Gibson W, Peacock L, Ferris V, Fischer K, Livingstone J, Thomas J, Bailey M. Genetic recombination between human and animal parasites creates novel strains of human pathogen. PLoS Negl Trop Dis. 2015; 9:e0003665. [PubMed: 25816228]

Guther ML, Urbaniak MD, Tavendale A, Prescott A, Ferguson MA. High-confidence glycosome proteome for procyclic form Trypanosoma brucei by epitope-tag organelle enrichment and SILAC proteomics. J Proteome Res. 2014; 13:2796–2806. [PubMed: 24792668]

Herbert WJ, Lumsden WH. Trypanosoma brucei: a rapid “matching” method for estimating the host’s parasitemia. Exp Parasitol. 1976; 40:427–431. [PubMed: 976425]

Jensen BC, Ramasamy G, Vasconcelos EJ, Ingolia NT, Myler PJ, Parsons M. Extensive stage-regulation of translation revealed by ribosome profiling of Trypanosoma brucei. BMC Genomics. 2014; 15:911. [PubMed: 25331479]

Kremer JR, Mastronarde DN, McIntosh JR. Computer visualization of three-dimensional image data using IMOD. J Struct Biol. 1996; 116:71–76. [PubMed: 8742726]

Magez S, Schwegmann A, Atkinson R, Claes F, Drennan M, De Baetselier P, Brombacher F. The role of B-cells and IgM antibodies in parasitemia, anemia, and VSG switching in Trypanosoma brucei-infected mice. PLoS Pathog. 2008; 4:e1000122. [PubMed: 18688274]

Mantel PY, Hoang AN, Goldowitz I, Potashnikova D, Hamza B, Vorobjev I, Ghiran I, Toner M, Irimia D, Ivanov AR, et al. Malaria-infected erythrocyte-derived microvesicles mediate cellular communication within the parasite population and with the host immune system. Cell Host Microbe. 2013; 13:521–534. [PubMed: 23684304]

Marcilla A, Martin-Jaular L, Trelis M, de Menezes-Neto A, Osuna A, Bernal D, Fernandez-Becerra C, Almeida IC, Del Portillo HA. Extracellular vesicles in parasitic diseases. J Extracell Vesicles. 2014; 3:25040. [PubMed: 25536932]

Mony BM, MacGregor P, Ivens A, Rojas F, Cowton A, Young J, Horn D, Matthews K. Genome-wide dissection of the quorum sensing signalling pathway in Trypanosoma brucei. Nature. 2014; 505:681–685. [PubMed: 24336212]

Naessens J. Bovine trypanotolerance: A natural ability to prevent severe anaemia and haemophagocytic syndrome? Int J Parasitol. 2006; 36:521–528. [PubMed: 16678182]

Oberholzer M, Langousis G, Nguyen HT, Saada EA, Shimogawa MM, Jonsson ZO, Nguyen SM, Wohlschlegel JA, Hill KL. Independent analysis of the flagellum surface and matrix proteomes provides insight into flagellum signaling in mammalian-infectious Trypanosoma brucei. Mol Cell Proteomics. 2011; 10:M111010538.

Oberholzer M, Lopez MA, McLelland BT, Hill KL. Social Motility in African Trypanosomes. PLoS pathogens. 2010; 6

Oli MW, Cotlin LF, Shiflett AM, Hajduk SL. Serum resistance-associated protein blocks lysosomal targeting of trypanosome lytic factor in Trypanosoma brucei. Eukaryot Cell. 2006; 5:132–139. [PubMed: 16400175]

Panigrahi AK, Ogata Y, Zikova A, Anupama A, Dalley RA, Acestor N, Myler PJ, Stuart KD. A comprehensive analysis of Trypanosoma brucei mitochondrial proteome. Proteomics. 2009; 9:434–450. [PubMed: 19105172]

Proto WR, Castanys-Munoz E, Black A, Tetley L, Moss CX, Juliano L, Coombs GH, Mottram JC. Trypanosoma brucei metacaspase 4 is a pseudopeptidase and a virulence factor. J Biol Chem. 2011; 286:39914–39925. [PubMed: 21949125]

Regev-Rudzki N, Wilson DW, Carvalho TG, Sisquella X, Coleman BM, Rug M, Bursac D, Angrisano F, Gee M, Hill AF, et al. Cell-cell communication between malaria-infected red blood cells via exosome-like vesicles. Cell. 2013; 153:1120–1133. [PubMed: 23683579]

Remis JP, Wei D, Gorur A, Zemla M, Haraga J, Allen S, Witkowska HE, Costerton JW, Berleman JE, Auer M. Bacterial social networks: structure and composition of Myxococcus xanthus outer membrane vesicle chains. Environ Microbiol. 2014; 16:598–610. [PubMed: 23848955]

Rifkin MR, Landsberger FR. Trypanosome variant surface glycoprotein transfer to target membranes: a model for the pathogenesis of trypanosomiasis. Proc Natl Acad Sci U S A. 1990; 87:801–805. [PubMed: 2300563]

Salmon D, Vanwalleghem G, Morias Y, Denoeud J, Krumbholz C, Lhomme F, Bachmaier S, Kador M, Gossmann J, Dias FB, et al. Adenylate cyclases of Trypanosoma brucei inhibit the innate immune response of the host. Science. 2012; 337:463–466. [PubMed: 22700656]

Schepilewsky E. Fadenförmige Anhängsel bei den Trypanosomen. Zentralblatt fur Bakteriologie, Parasitenkunde, Infektionskrankheiten und Hygiene. 1912; 65:79–83.

Schorey JS, Cheng Y, Singh PP, Smith VL. Exosomes and other extracellular vesicles in host-pathogen interactions. EMBO Rep. 2015; 16:24–43. [PubMed: 25488940]

Silverman JM, Clos J, de'Oliveira CC, Shirvani O, Fang Y, Wang C, Foster LJ, Reiner NE. An exosome-based secretion pathway is responsible for protein export from Leishmania and communication with macrophages. J Cell Sci. 2010; 123:842–852. [PubMed: 20159964]

Stephens NA, Hajduk SL. Endosomal localization of the serum resistance-associated protein in African trypanosomes confers human infectivity. Eukaryot Cell. 2011; 10:1023–1033. [PubMed: 21705681]

Stijlemans B, Cnops J, Naniima P, Vaast A, Bockstal V, De Baetselier P, Magez S. Development of a pHrodo-based assay for the assessment of in vitro and in vivo erythrophagocytosis during experimental trypanosomosis. PLoS Negl Trop Dis. 2015; 9:e0003561. [PubMed: 25742307]

Sykes S, Szempruch A, Hajduk S. The krebs cycle enzyme alpha-ketoglutarate decarboxylase is an essential glycosomal protein in bloodstream African trypanosomes. Eukaryot Cell. 2015; 14:206–215. [PubMed: 25416237]

Truc P, Buscher P, Cuny G, Gonzatti MI, Jannin J, Joshi P, Juyal P, Lun ZR, Mattioli R, Pays E, et al. Atypical human infections by animal trypanosomes. PLoS Negl Trop Dis. 2013; 7:e2256. [PubMed: 24069464]

Twu O, de Miguel N, Lustig G, Stevens GC, Vashisht AA, Wohlschlegel JA, Johnson PJ. Trichomonas vaginalis exosomes deliver cargo to host cells and mediate hostratioparasite interactions. PLoS Pathog. 2013; 9:e1003482. [PubMed: 23853596]

Vanhamme L, Paturiaux-Hanocq F, Poelvoorde P, Nolan DP, Lins L, Van Den Abbeele J, Pays A, Tebabi P, Van Xong H, Jacquet A, et al. Apolipoprotein L-I is the trypanosome lytic factor of human serum. Nature. 2003; 422:83–87. [PubMed: 12621437]

Vickerman K, Luckins AG. Localization of variable antigens in the surface coat of Trypanosoma brucei using ferritin conjugated antibody. Nature. 1969; 224:1125–1126. [PubMed: 5353729]

Vidal M, Hoekstra D. In vitro fusion of reticulocyte endocytic vesicles with liposomes. J Biol Chem. 1995; 270:17823–17829. [PubMed: 7629083]

Webb H, Carnall N, Vanhamme L, Rolin S, Van Den Abbeele J, Welburn S, Pays E, Carrington M. The GPI-phospholipase C of Trypanosoma brucei is nonessential but influences parasitemia in mice. J Cell Biol. 1997; 139:103–114. [PubMed: 9314532]

Wood CR, Rosenbaum JL. Ciliary ectosomes: transmissions from the cell's antenna. Trends Cell Biol. 2015; 25:276–285. [PubMed: 25618328]

Wright KA, Lumsden WH, Hales H. The formation of filopodium-like processes by Trypanosoma (Trypanozoon) brucei. J Cell Sci. 1970; 6:285–297. [PubMed: 4907042]

Xong HV, Vanhamme L, Chamekh M, Chimfwembe CE, Van Den Abbeele J, Pays A, Van Meirvenne N, Hamers R, De Baetselier P, Pays E. A VSG expression site-associated gene confers resistance to human serum in Trypanosoma rhodesiense. Cell. 1998; 95:839–846. [PubMed: 9865701]

Yanez-Mo M, Siljander PR, Andreu Z, Zavec AB, Borras FE, Buzas EI, Buzas K, Casal E, Cappello F, Carvalho J, et al. Biological properties of extracellular vesicles and their physiological functions. J Extracell Vesicles. 2015; 4:27066. [PubMed: 25979354]

Zomer A, Maynard C, Verweij FJ, Kamermans A, Schafer R, Beerling E, Schiffelers RM, de Wit E, Berenguer J, Ellenbroek SI, et al. In Vivo imaging reveals extracellular vesicle-mediated phenocopying of metastatic behavior. Cell. 2015; 161:1046–1057. [PubMed: 26000481]

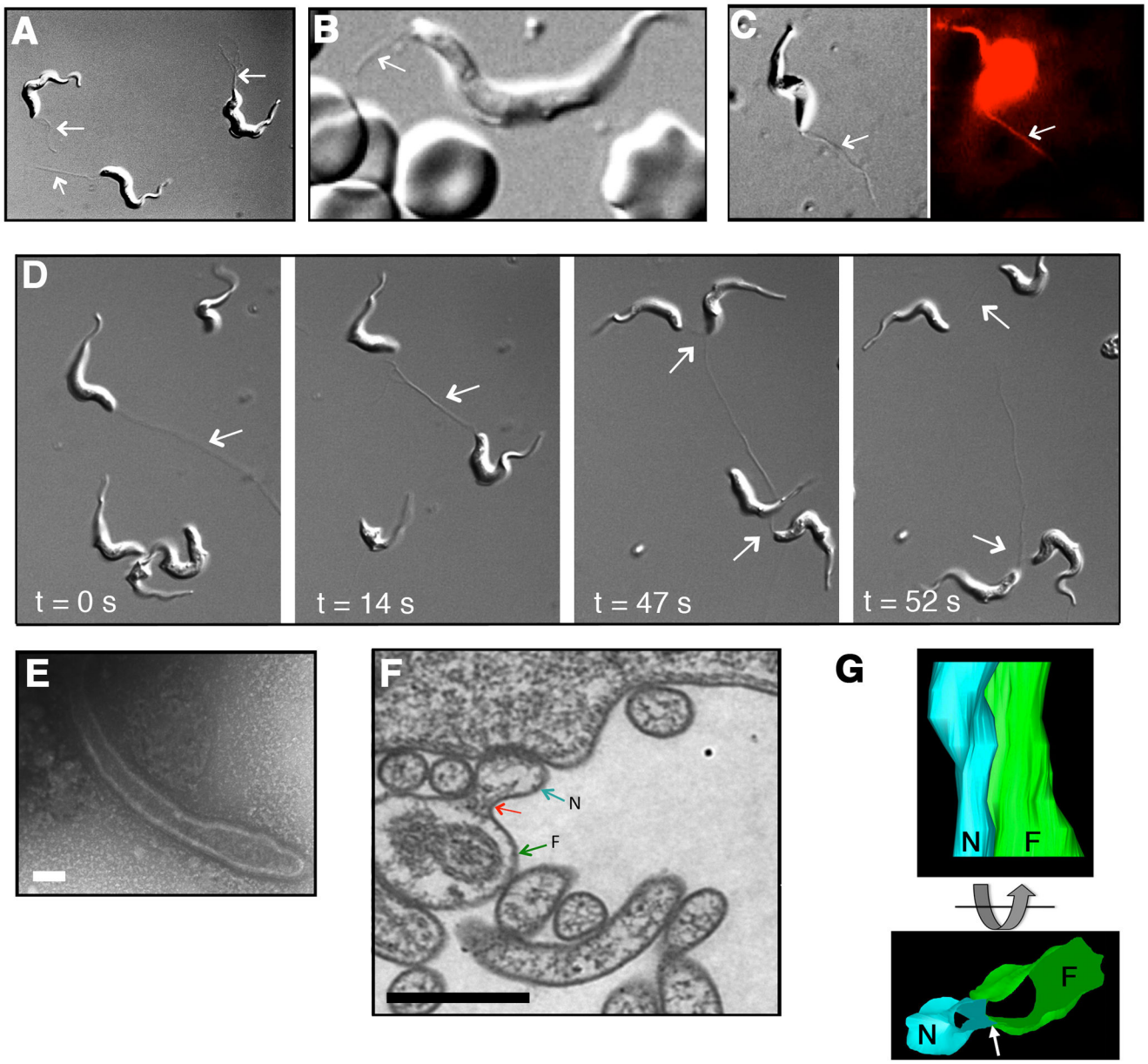

Figure 1. Dynamics and flagellar formation of membrane nanotubes

(**A**) Nanotube formation was visualized by DIC microscopy. Arrows indicate nanotubes. (**B**) Nanotubes on *T. brucei* in infected mouse blood. Arrow indicates nanotube. (**C**) Nanotubes were labeled by R18. Left and right panels are consecutive frames from DIC and fluorescence video microscopy, respectively (see Movie S1 and S2). (**D**) Live cell imaging revealed membrane nanotube dynamics, interactions with multiple cells in sequential DIC frames (see Movie S3). (**E**) Nascent nanotube visualized by negative stain TEM (bar = 100 nm). (**F**) TEM thin section showed flagellar membrane (green arrow, F) budding (red arrow) into nanotube (blue arrow, N) (bar = 500 nm). (**G**) Reconstruction of serial TEM thin sections into a 3D model showed tubulation (blue) of flagellar membrane (green). Arrow

indicates nanotube budding point (see Movie S4). See also Figures S1A–D, Movie S1, S2, S3, and S4.

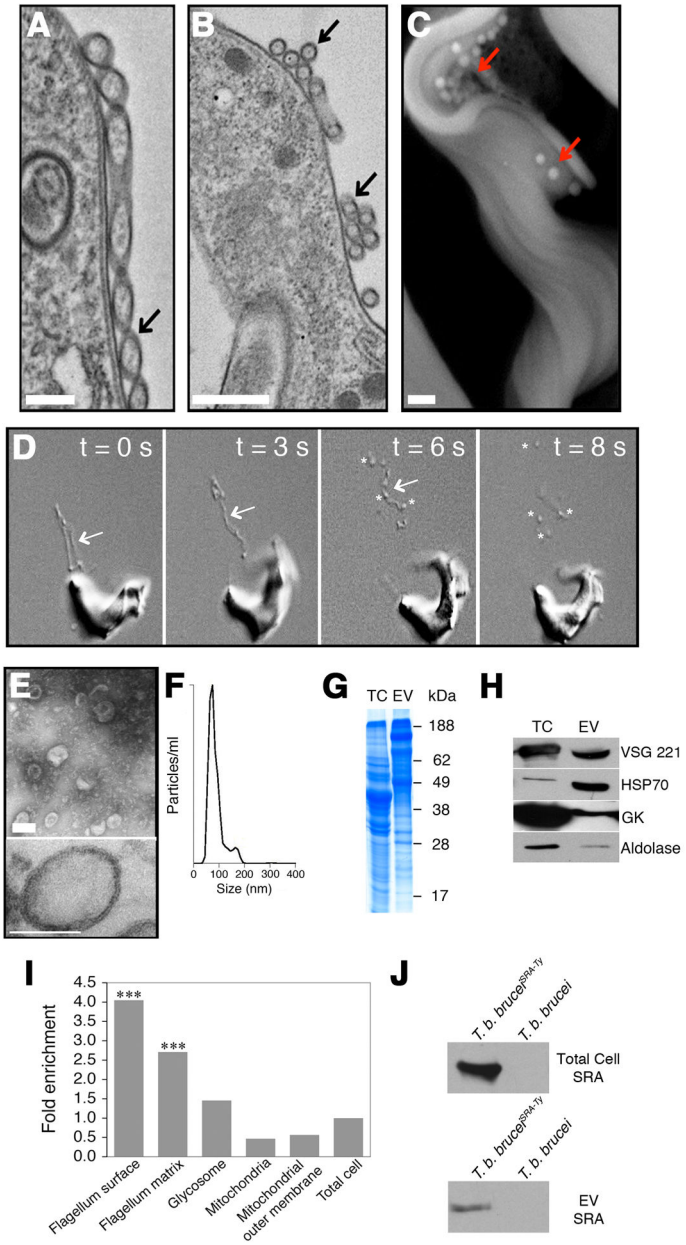

Figure 2. Nanotubes vesicularize into EVs

(**A**) TEM of a nanotube (black arrow) (bar = 400 nm) and (**B**) spherical units (black arrow) (bar = 500 nm). (**C**) Free EVs (red arrows) at the trypanosome surface visualized by SEM (bar = 400 nm). (**D**) Successive DIC video frames of nanotubes (arrows) dissociating into free EVs (asterisks) (see Movie S5). (**E, upper panel**) Negative stain TEM of purified EVs (bar = 100 nm). (**E, lower panel**) TEM thin section of purified EVs (bar = 100 nm). (**F**) Nanoparticle tracking analysis of EVs. (**G**) EV proteins visualized by SDS-PAGE (total cell, TC). (**H**) Western blotting of EVs with anti-VSG, HSP70, glycerol kinase and aldolase. (**I**) Analysis of the EV proteome for relative enrichment with flagellar surface, flagellar matrix, glycosome, mitochondria and mitochondrial outer membrane proteins in relation to the total

cell proteome (***, $p < 0.001$). (**J**) Western blot of total cell and EVs from *T. b. brucei*$^{SRA\text{-}Ty}$. See also Figures S1E–F, Movie S5, Table S1 and S2.

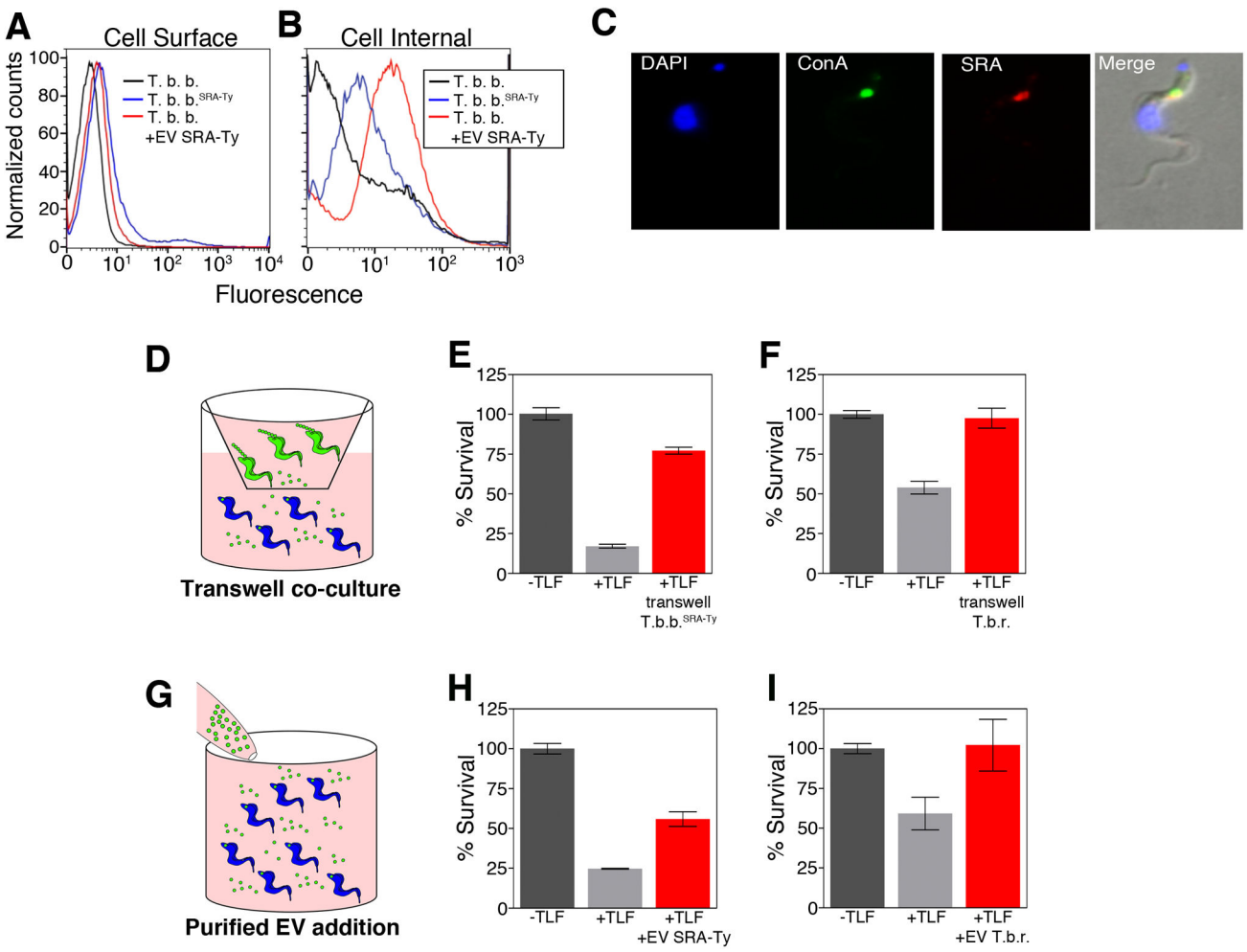

Figure 3. EVs transfer TLF resistance

(**A**) Flow cytometry of fixed *T. brucei* (black), *T. b. brucei*$^{SRA\text{-}Ty}$ (blue) and *T. brucei* treated with SRA containing EVs (red). (**B**) Flow cytometry of fixed and permeabilized *T. brucei* (black), *T. b. brucei*$^{SRA\text{-}Ty}$ (blue) and *T. brucei* treated with SRA containing EVs (red). (**C**) Fluorescence microscopy of *T. brucei* treated with EVs containing SRA. ConA showed internalization and co-localization in the endocytic pathway. (**D**) Diagram of transwell co-culture of *T. brucei* with *T. b. brucei*$^{SRA\text{-}Ty}$ or *T. b. rhodesiense*. (**E & F**) TLF overnight survival assays. *T. b. brucei* not treated with TLF (negative control) (dark grey) *T. b. brucei* treated with TLF (positive control) (light grey). **(E)** Co-culture of *T. b. brucei* with *T. b. brucei*$^{SRA\text{-}Ty}$ (red) and **(F)** co-culture of *T. b. brucei* with *T. b. rhodesiense* (red). (**G**) Diagram depicting addition of EVs from *T. b. brucei*$^{SRA\text{-}Ty}$ or *T. b. rhodesiense* to *T. b. brucei*. (**H & I**) TLF overnight survival assays. *T. b. brucei* not treated with TLF (negative control) (dark grey) *T. b. brucei* treated with TLF (positive control) (light grey). **(H)** Addition of EVs purified from *T. b. brucei*$^{SRA\text{-}Ty}$ (red) and (**I**) addition of EVs purified from *T. b. rhodesiense* (red). Bars represent the mean ± SEM for three experiments. See also Figures S2A–E, S4 and S5.

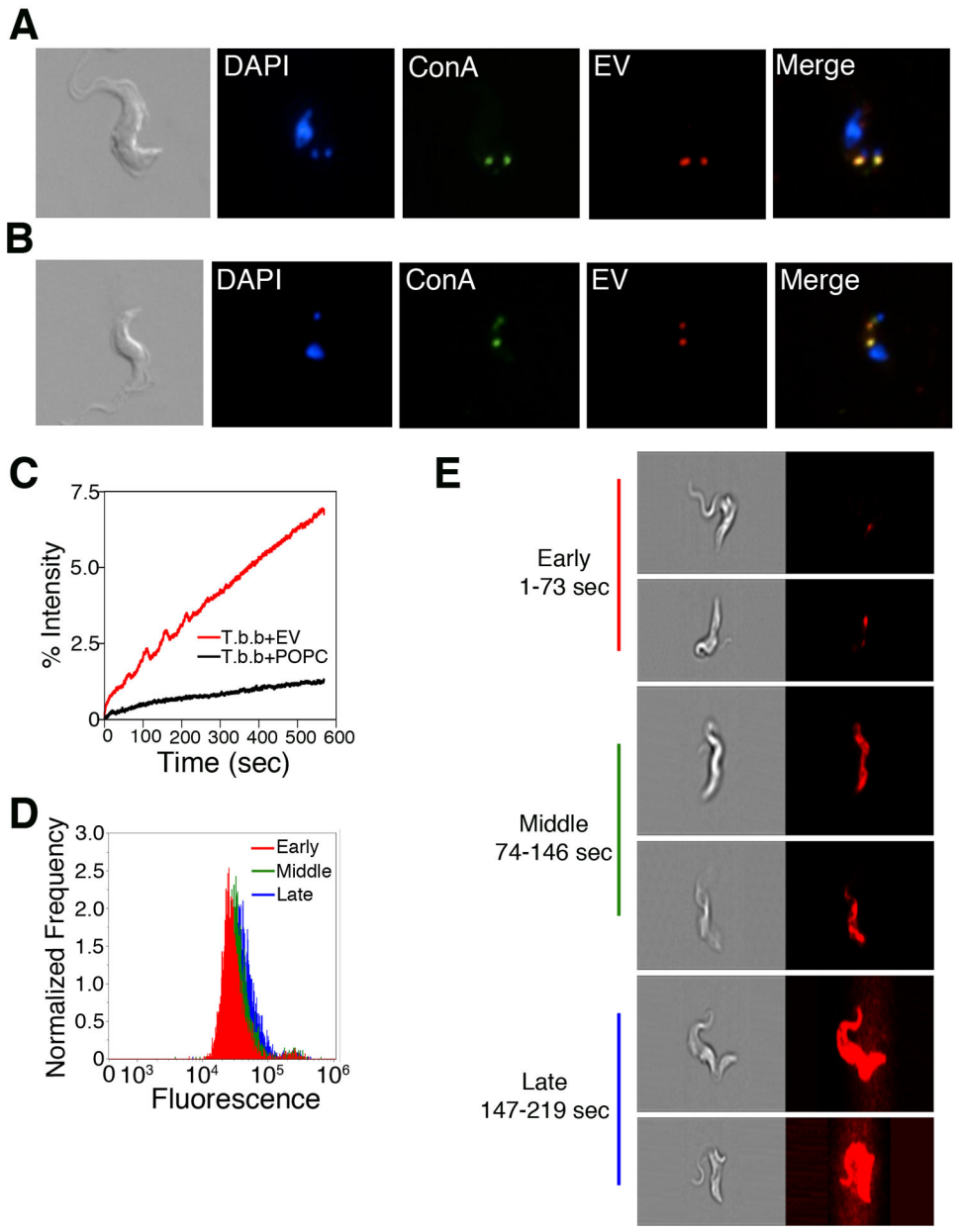

Figure 4. EVs interact with *T. brucei* at the flagellar pocket and are endocytosed

(**A & B**) Fluorescence microscopy of *T. brucei* treated with Alexa-594 labeled EVs. **(A)** EVs localized with ConA to the flagellar pocket at 3°C. (**B)** EVs localized with ConA in the endocytic pathway at 37°C. (**C**) Membrane fusion was measured by fluorescence dequenching of R18-labeled EVs (red) with *T. brucei*. Fusion did not occur when *T. brucei* was treated with R18-labeled POPC (black). (**D**) ImageStream flow cytometry showed fluorescence dequenching occurred across the entire cell population with increasing intensity in a time dependent manner (1–73 sec “early”, red; 74–146 sec “middle”, green; 147–219 sec “late”, blue). (**E**) Imaging of individual cells during the ImageStream analysis showed that during early time cells showed a discreet fluorescent puncta at the posterior end

of the cell with fluorescent rapidly distributing across the cell resulting in fully fluorescent cells in later times. See also Figures S3A–K and S4A–C.

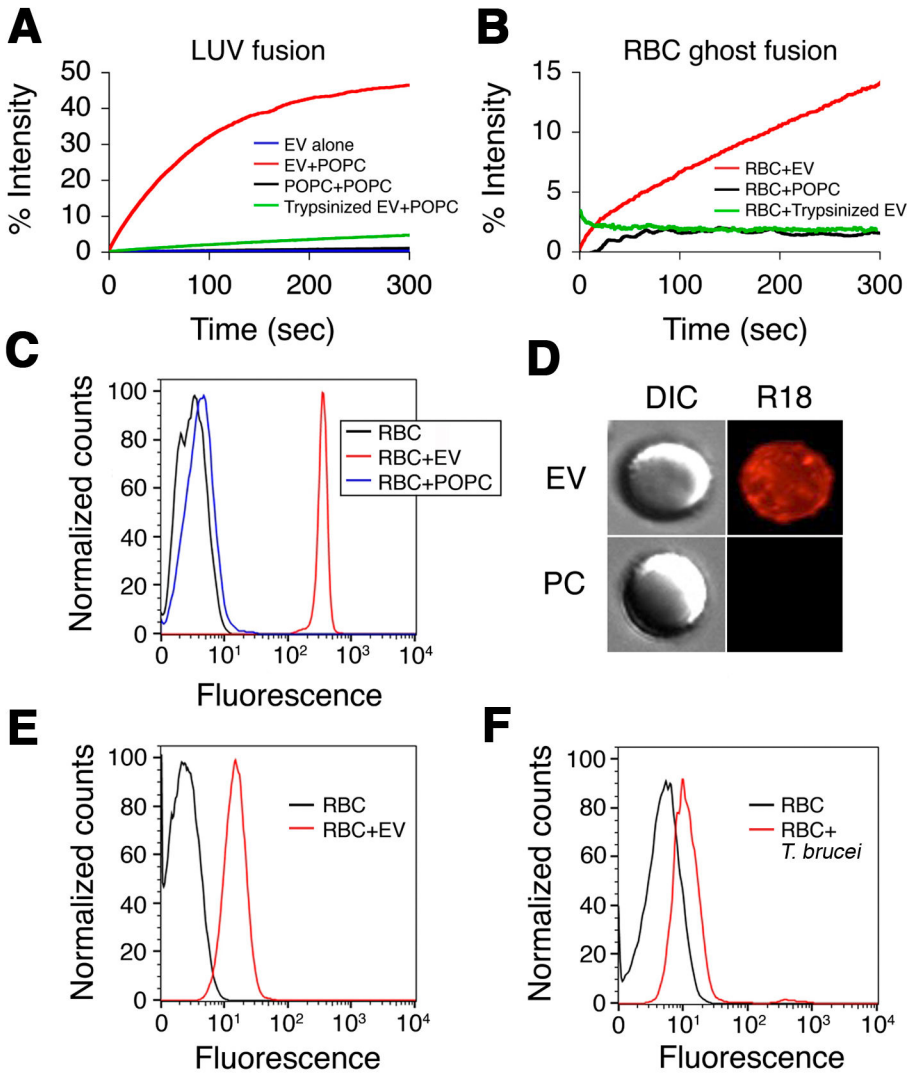

Figure 5. Trypanosome EVs fuse with erythrocytes

(**A**) Membrane fusion was measured by fluorescence dequenching of R18-labeled EVs (EV + POPC, red; EVs alone, blue; R18-labeled POPC + POPC, black). Trypsinization of EV ablates fusion with POPC LUV (green). (**B**) EVs (red), but not POPC LUV (black) or trypsinized EVs (green), fuse with human erythrocyte ghosts. (**C**) Intact human erythrocytes (black) were incubated with R18-labeled EVs (red) or R18-labeled POPC LUV (blue) and analyzed by flow cytometry. (**D**) Intact human erythrocytes were incubated with R18-labeled EVs or R18-labeled POPC LUV (PC) and visualized by fluorescence microscopy. (**E**) Alexa-Fluor 488-labeled EVs were incubated with intact human erythrocytes and analyzed by flow cytometry (black, untreated erythrocytes; red, erythrocytes + EVs). (**F**) Human erythrocytes were incubated overnight in transwells with or without R18-labeled BF *T. brucei* and analyzed by flow cytometry (black, erythrocytes alone; red, erythrocytes + R18-labeled trypanosomes). See also Figure S5A–D.

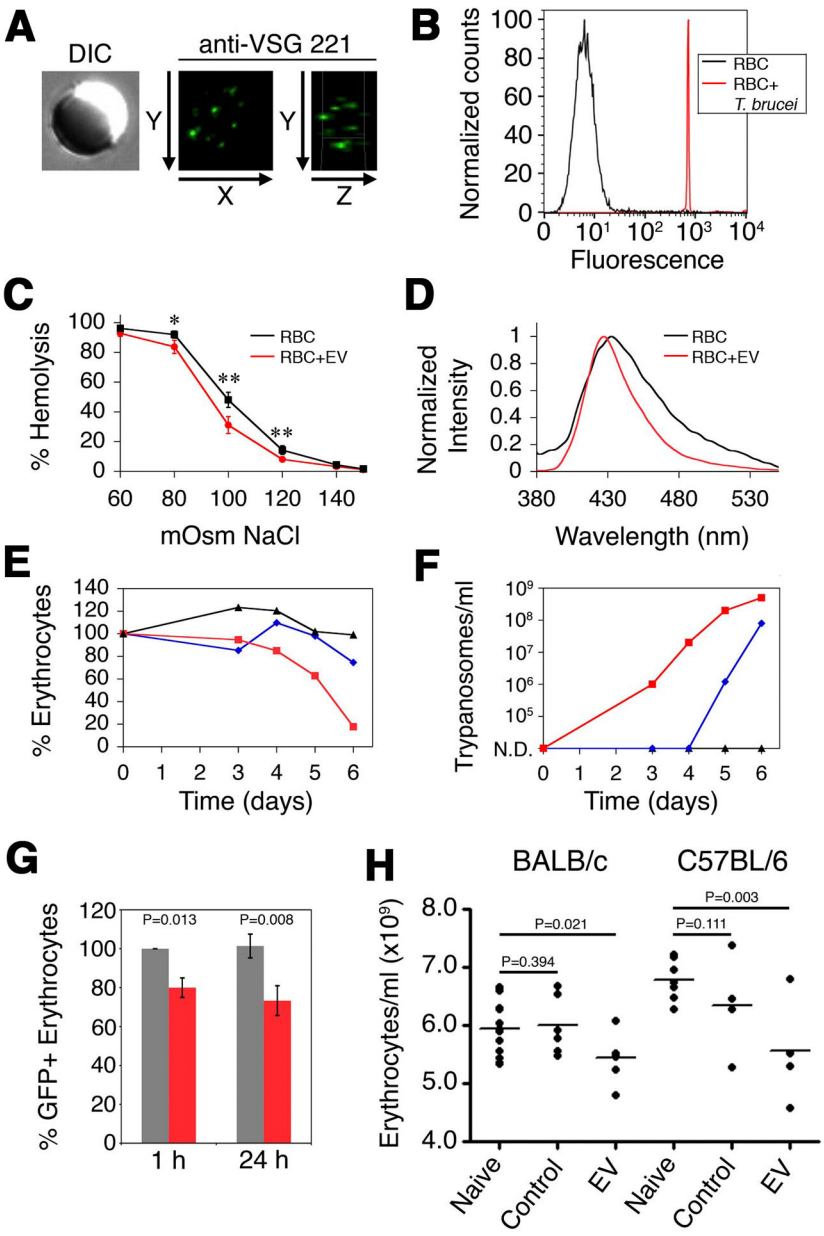

Figure 6. EVs alter erythrocyte physicochemical properties and stimulate clearance

(**A**) Erythrocytes were incubated with EVs, probed with anti-VSG 221 and visualized by fluorescence microscopy. (**B**) Erythrocytes were incubated in transwells in the presence (red) or absence (black) of *T. brucei*, probed with anti-VSG 221 and analyzed by flow cytometry. (**C**) Erythrocyte lysis was measured by quantifying hemoglobin concentration in supernatant (black, untreated erythrocytes; red, erythrocytes + EVs) (*, $p < 0.05$; **, $p \leq 0.005$). Scale bars represent the mean ± SEM for four experiments. (**D**) Laurdan emission spectra of erythrocytes alone (black) or treated with EVs (red). (**E**) Anemia in *T. brucei*-infected mice was followed by hemocytometer counts, normalized to pre-infection, in a heavily infected mouse (red), moderately infected mouse (blue) and a mouse with undetectable parasitemia (black). (**F**) Parasitemia of the mice shown in panel E. (**G**) Mouse

erythrocytes containing GFP were incubated with (red) or without (grey) purified EVs and injected into the tail vein of naive mice. GFP-erythrocytes were quantified by flow cytometry. Scale bars represent the mean ± SEM for four experiments. (**H**) Purified EVs were intravenously injected into naive mice and erythrocytes were quantified 1 h post injection. P-values were calculated by one-tailed student T-test. See also Figures S5.